Supporting Information

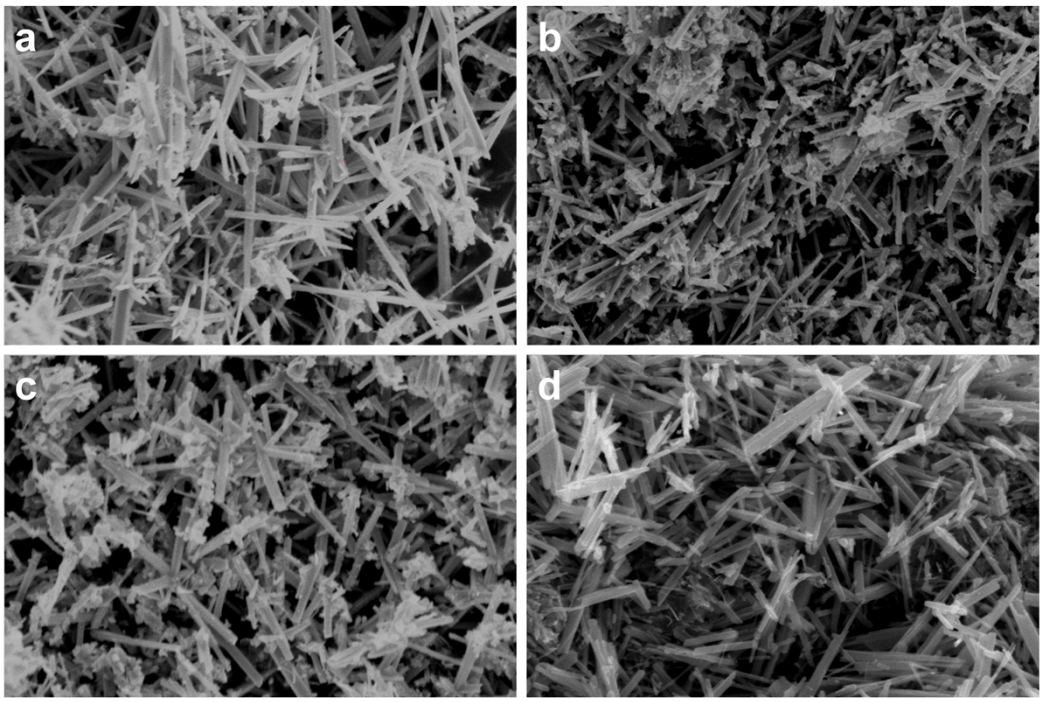

Figure S1. SEM images of OMS-La, OMS-Gd, OMS-Lu and OMS.

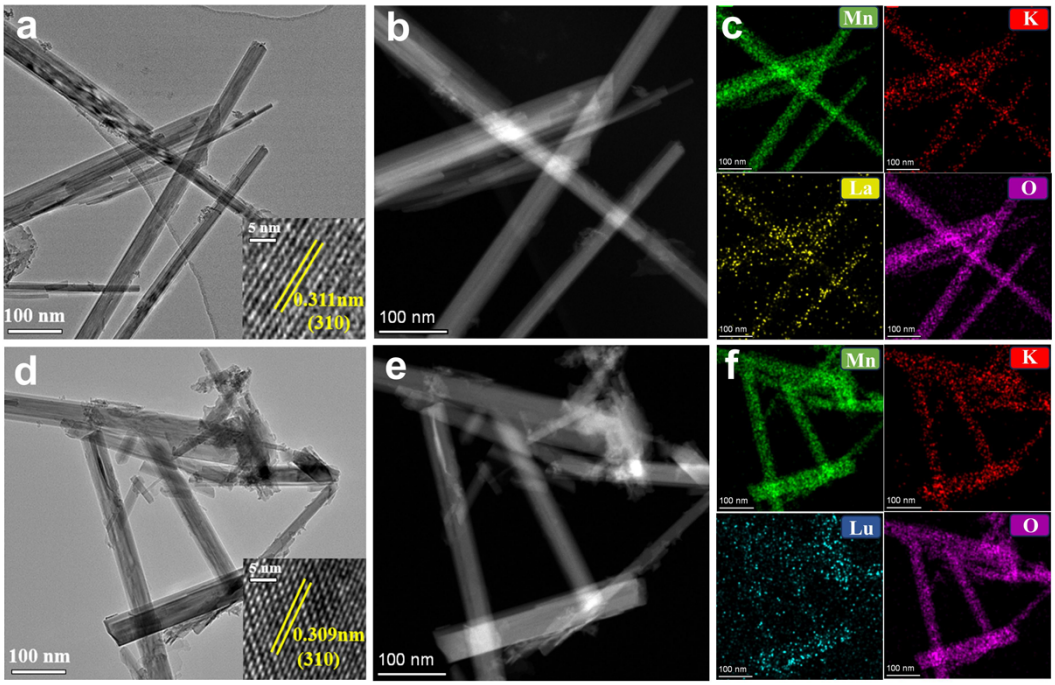

Figure S2. OMS-La: a) TEM image (illustrated by lattice fringe diagram) and b,c) mapping image. OMS-Lu: d) TEM image(illustrated by lattice fringe diagram) and e,f) mapping image.

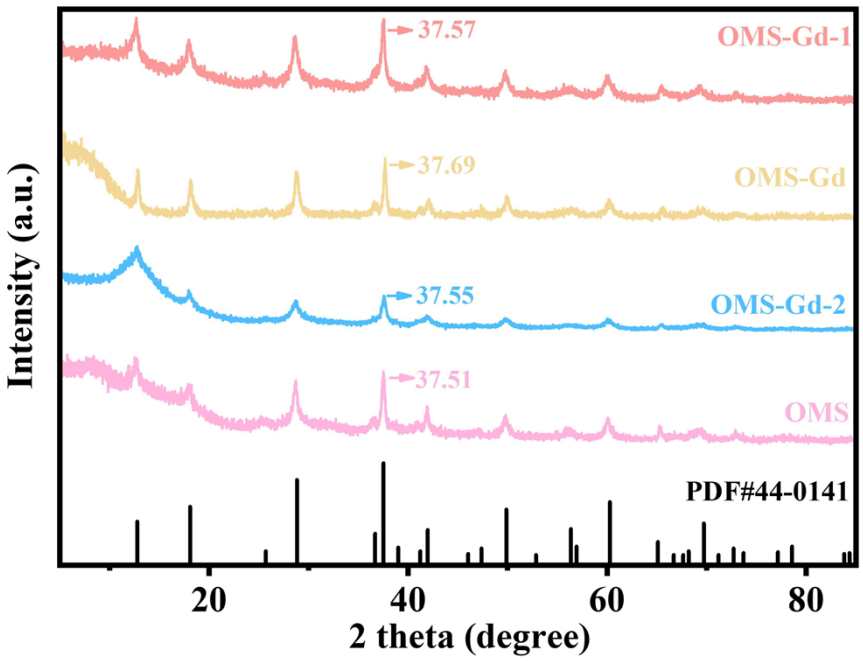

Figure S3. XRD patterns of OMS doped with different gadolinium ion contents

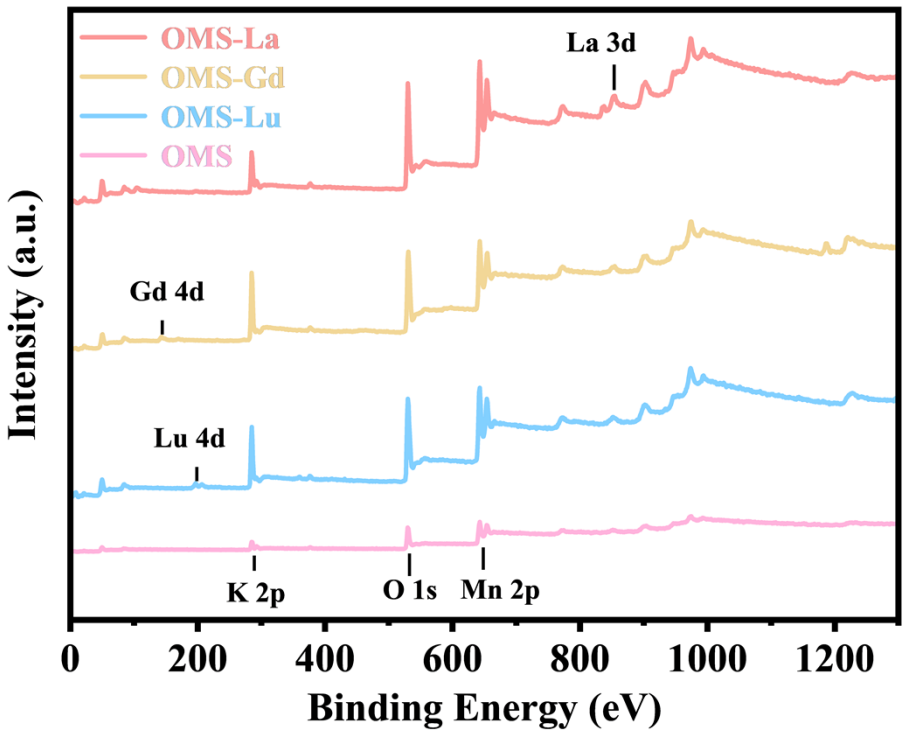

Figure S4. XPS full spectrum of OMS and other lanthanide doped catalysts.

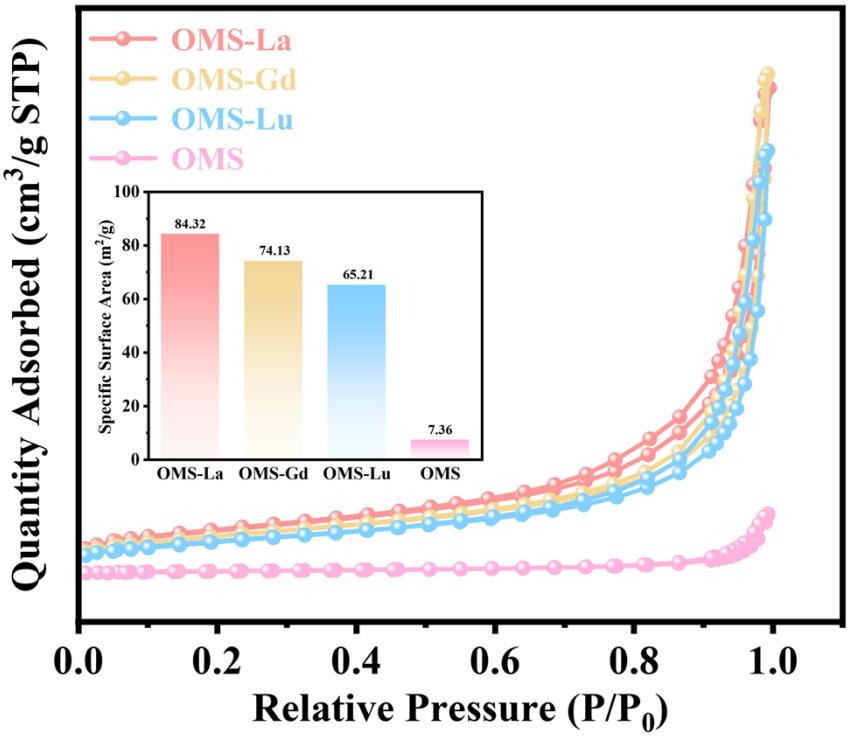

Figure S5. The specific surface area of OMS-La, OMS-Gd, OMS-Lu and OMS (The illustration is a statistical diagram of specific surface area).

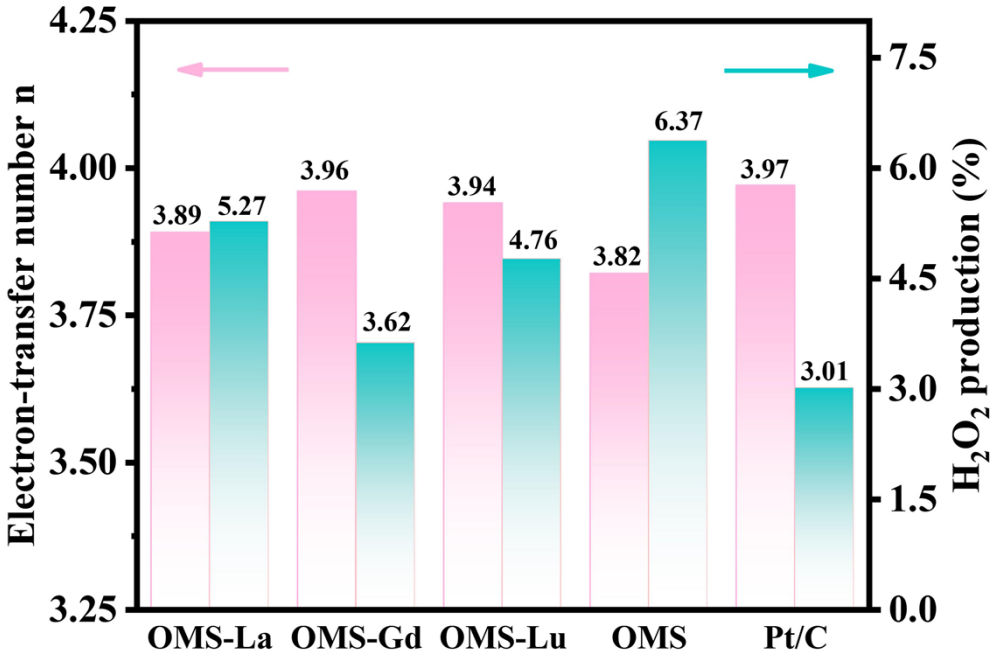

Figure S6. Columnar diagram of electron transfer number and H_2O_2 yield.

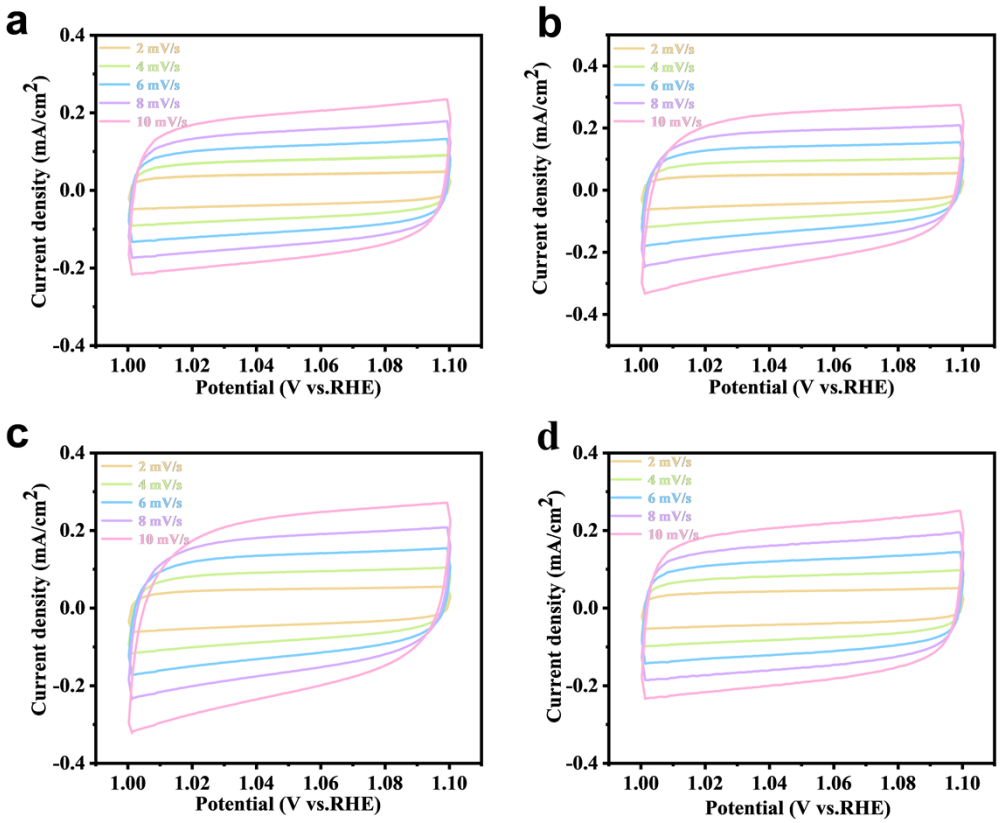

Figure S7. Cyclic voltammograms plots at different scanning rates of a) OMS-La, b) OMS-Gd, c) OMS-Lu, and d) OMS.

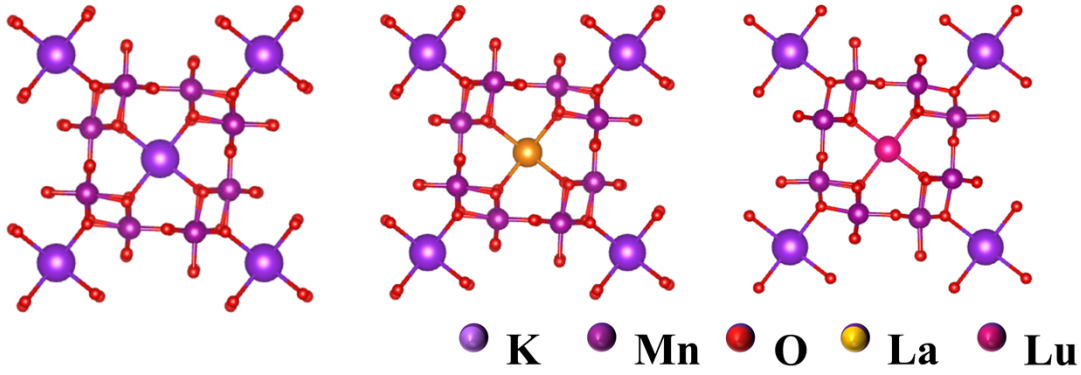

Figure S8. The theoretical models of OMS, OMS-La and OMS-Lu.

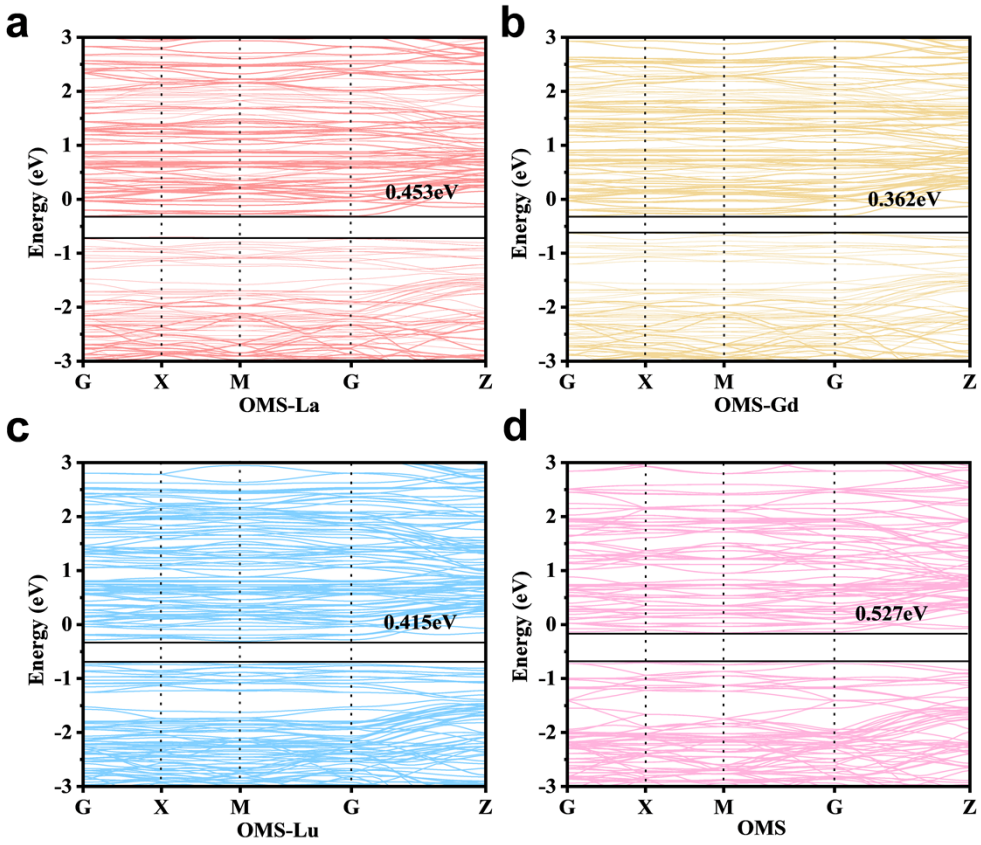

Figure S9. The schematic diagram of band gap.

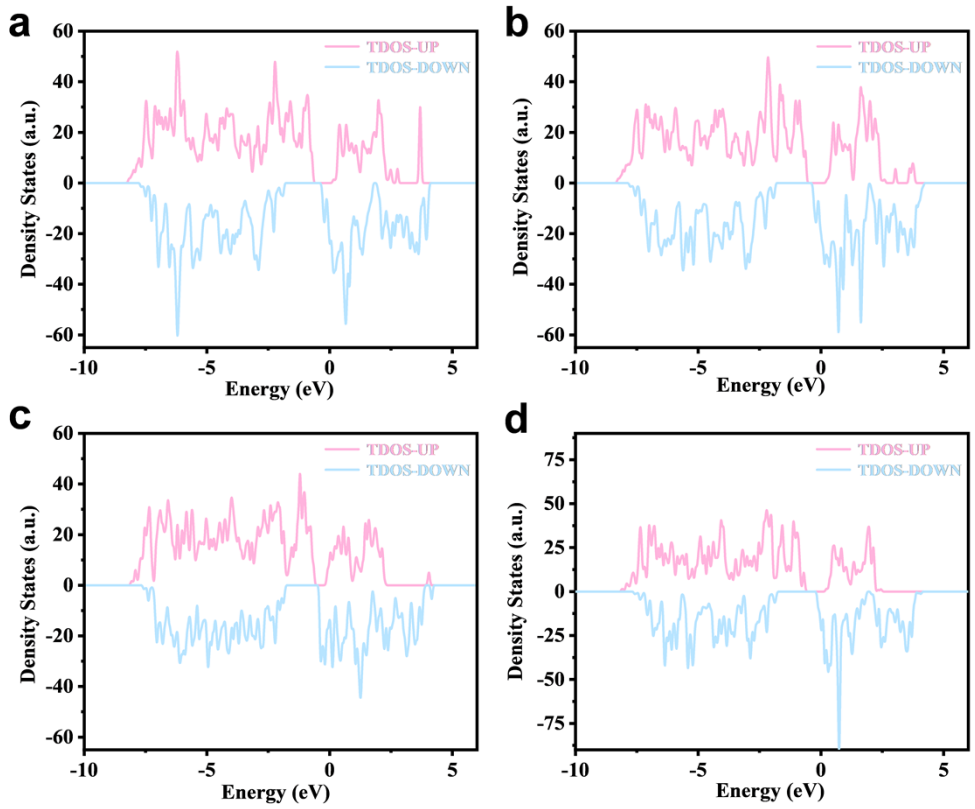

Figure S10. TDOS of a) OMS-La, b) OMS-Gd, c) OMS-Lu and d) OMS-2.

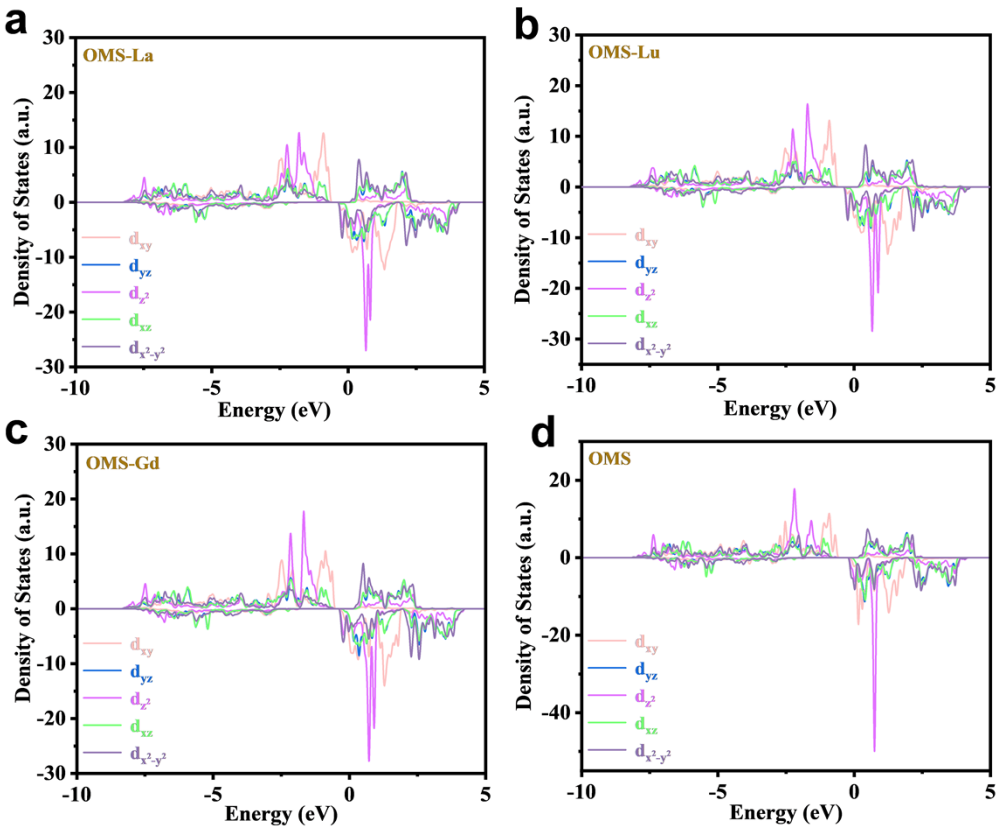

Figure S11. Mn PDOS of a) OMS-La, b) OMS-Gd, c) OMS-Lu and d) OMS.

Table S1. The atomic ratio of sample elements in the catalyst as determined by ICP testing(X denotes lanthanide metal ions).

Catalyst	K:Mn	X:Mn
OMS-La	0.146:1	0.076:1
OMS-Gd	0.126:1	0.013:1
OMS-Lu	0.128:1	0.018:1
OMS	0.178:1	

Table S2. The relative contents of Mn^{3+} and Mn^{4+} in OMS-Gd were calculated.

Catalyst	Mn^{3+} Contents(%)	Mn^{4+} Contents(%)
OMS-La	40	60
OMS-Gd	57	43
OMS-Lu	44	56
OMS	32	68

Table S3. The calculation of electron occupation number of eg orbital d_z^2 energy level and $d_{x^2-y^2}$ energy level of four catalysts.

	OMS-La (eV)	OMS-Gd (eV)	OMS-Lu (eV)	OMS (eV)
$d_{x^2-y^2}$	0.139	0.162	0.145	0.133
d_z^2	0.214	0.228	0.218	0.209

Table S4. The calculation results of $d_{x^2-y^2}$ energy level and d_z^2 energy level in e_g orbit of four catalysts.

	OMS-La (eV)	OMS-Gd (eV)	OMS-Lu (eV)	OMS (eV)
$d_{x^2-y^2}$	-2.09	-2.06	-2.08	-2.22
d_z^2	-2.67	-2.64	-2.65	-2.77

Table S5. Comparison of some recently reported ORR electrocatalysts performance.

Catalyst	ORR $E_{1/2}$ (V)	Reference
OMS-Gd	0.83	This work
CCSO/NC-2	0.75	Adv. Mater. 2023, 35, 2303488.
NIS/$NiFe_2O_4$	0.81	Adv. Mater. 2022, 34, 2110172.
Ir@Co_3O_4	0.75	Adv. Funct. Mater. 2022, 32, 2111989.
CoxP@NP-C	0.82	Angew. Chem. Int., Ed. 2020, 59, 21360.
P-NCO/NCN-CF@CC	0.83	Adv. Funct. Mater. 2023, 33, 2302883.
CoP/CoO@MNC-CNT	0.838	Small. 2023, 19, 2206341.
$Ce_{0.05}$─N─C/Cu_{clu}	0.79	Adv. Funct. Mater. 2025, e15095.
EuCo-NC	0.824	J. Electroanal. Chem. 2025, 983, 119031.
(a+δ)-Mn11	0.726	Catal. Sci. Technol. 2020, 10,7352–7364.
ACMO	0.81	Chem sus chem. 2022, 15, e202200612.
Hollow α-MnO_2	0.80	Inorg. Chem. Commun. 2022,146, 110143.
NiFeMn	0.81	J. Energy Storage. 2023, 74, 109350.
U-MnO_2/PSNC	0.814	Ceram. Int. 2022, 48, 6506–6511.